Journal of Alloys and Compounds 509 (2011) 6829–6833

Contents lists available at ScienceDirect

Journal of Alloys and Compounds

journal homepage: www.elsevier.com/locate/jallcom

Phase-separation-induced self-assembly of controllable $PbTiO_3$ nanodots on Si substrates

Kui Cheng, Jinna Li, Wenjian Weng*, Ming Luo, Piyi Du, Ge Shen, Gaorong Han

Department of Materials Science & Engineering, State Key laboratory of Silicon Materials, Zhejiang University, Zheda Road 38, Hangzhou, Zhejiang 310027, PR China

ARTICLE INFO

Article history:
Received 20 December 2010
Received in revised form 16 March 2011
Accepted 17 March 2011
Available online 27 March 2011

Keywords:
$PbTiO_3$
PSIA
Nanodots on substrate

ABSTRACT

In this work, a phase-separation-induced self-assembly (PSIA) approach was developed to prepare $PbTiO_3$ nanodots on substrates. Lead titanate nanodots on Si wafer were obtained through Marangoni instability induced phase separation and following heat-treatment. It was found that acetylacetone added in the precursor played important roles not only in the incorporation of Pb into the nanodots, but also in the phase separation process. The size and density of PT nanodots could be controlled through the concentrations of precursor and phase separation adjuster, i.e., tetrabutyl-titanate and polyvinylpyrrolidone. The nanodots size and density were from 10 nm to ~100 nm and from 0.5×10^{10} dots/cm^{-2} to 4.6×10^{10} dots/cm^{-2} respectively. Such preparation provides a simple way to prepare titanate nanodots on substrate.

1. Introduction

Ceramics with ABO_3 formula have been widely studied in memories, transducers and many other fields owing to their excellent dielectricity, ferroelectricity, piezoelectricity and other properties [1–3]. Many works have been carried out on lead-free ABO_3 ceramics due to both performance and environmental considerations [4–6]. Recently, with the development of high density memory devices, nanostructured ABO_3 ceramics are considered to be increasingly more important. Although lead-containing, lead titanate has been regarded as a good model system to explore the dependence of properties upon reduction in dimension and size [7–9].

Many works on nanostructured $PbTiO_3$ (PT) have been carried out. Lead titanate nanoparticles could be prepared by a vibro-milling technique [10], an oxidant peroxo method [11], a Pechini method [12] and a combustion synthesis [13]. Usually, these methods involve high temperature annealing processes that led to polycrystalline particles with a uniform spherical shape around 100 nm and sharp size distribution. The incorporation of such PT nanoparticles into micron-sized PT matrix was found to be able to improve the dielectric properties [14]. Many other nanostructure forms of PT were also reported: PT nanorods were synthesized through phase transformation of precursor $Pb_2Ti_2O_6$ nanorods [15]; PT nanorods arrays were prepared through liquid-phase deposition with the aid of anodic aluminum oxide template [16]; PT nanotubes were prepared by sol–gel method [17] and hydrothermal synthesis [18].

So far, in real application, most devices need nanostructured PT to deposit on substrates. Some researches focused on direct preparation of certain PT nanostructure on substrates so that they may act as a seeding layer in subsequent deposition. It was reported that even those nanosized grains in bottom nanostructured layer could acted as nucleation sites and thus be beneficial for further deposition of upper crystallized layers [19]. Lead titanate dots on substrate were derived directly from an uncontinuous thin film [20] or further treated by high temperature annealing [21]. Also, some bottom-up methods, including chemical solution deposition, sol–gel chemistry and microemulsion mediated synthesis [22–24], were adopted to prepare nanostructured PT on substrates. Ultrahigh density PT nanodots array on substrate through a microemulsion-assisted chemical solution deposition showed that the nanodots had well-defined epitaxy on the substrate and unique piezoresponse [25], and thus became much closer to real application in ferroelectric devices. Hence, a facile and reliable preparation of PT nanodots on substrates is very significant to further research and application.

Although sol–gel preparation of PT has been intensively studied [26–30], most of them focused on the phase purity and some other properties. In our previous work, a sol–gel based phase-separation-induced self-assembly (PSIA) route was proven to be effective in direct preparation of TiO_2 nanodots on substrates with controlled nanodot size and density [31,32]. Based on that, PT

* Corresponding author. Tel.: +86 571 87953787; fax: +86 571 87953787.
E-mail address: wengwj@zju.edu.cn (W. Weng).

0925-8388/$ – see front matter © 2011 Elsevier B.V. All rights reserved.
doi:10.1016/j.jallcom.2011.03.102

Table 1
Purity and origins of reagents.

Reagent	Purity (%)	Origin
Acetate trihydrate (CAS: 546-67-8)	≥99.5	Sinopharm Chemical
Acetylacetone (CAS: 81235-32-7)	>99	Lingfeng Chemical
Tetrabutyl-titanate (CAS: 5593-70-4)	>98	Sinopharm Chemical
Polyvinylpyrrolidone (CAS: 9003-39-8)	>99	Sinopharm Chemical
Absolute ethanol (CAS: 9003-99-0)	>99.7	Sinopharm Chemical

Table 2
Preparation conditions for different samples.

Sample	TBOT(mol/L)	PVP (g/L)	Pb:Hacac (molar ratio)
PT1	0.1	30	1:1.5
PT2	0.1	30	1:2
PT3	0.1	30	1:2.5
PT4	0.005	30	1:2
PT5	0.01	30	1:2
PT6	0.02	30	1:2
PT7	0.03	30	1:2
PT8	0.02	20	1:2
PT9	0.02	40	1:2

nanodots was also derived and showed enhanced field emission [33]. In this work, we looked into the formation of PT nanodots, and the influence of processing factors were characterized and discussed.

2. Experimental

All the information of reagents used was tabulated in Table 1. The precursor sol was first prepared through dissolution of lead acetate trihydrate ($Pb(OAc)_2{\cdot}3H_2O$), acetylacetone (Hacac), tetrabutyl-titanate (TBOT) and polyvinylpyrrolidone (PVP, K30) in absolute ethanol. The molar ratio of Pb:Ti (in $Pb(OAc)_2$ and TBOT respectively) was designed at 1:1. Such precursor was expected to be able to produce stoichiometric PT phase. Also, in order to control size and density of PT nanodots, varied TBOT, PVP and Hacac concentrations were designed, as tabulated in Table 2. The solution was stirred vigorously for 5 min at room temperature to be a homogeneous precursor sol with a total amount of 30 ml.

Si wafers were cut into small pieces (12 mm × 12 mm) to be substrates, ultrasonically cleaned in deionized water and dried in an oven held at 80 °C. After mounted on a spin-coater (Chemat Technology, KW-4A), a drop of precursor sol was dripped on substrate and spun at 8000 rpm for 40 s. Then, the coated substrate was annealed in a muffle furnace at 700 °C for 12 h, with a heating rate of 10 °C/min and a cooling rate of 1 °C/min.

The morphology and size distribution of PT nanodots were observed in a field-emission scanning electron microscope (FESEM, Hitachi S-4800). Before observation, a conductive gold layer was deposited on the surface. An image analysis software (DT2000) was used to characterize the size and distribution of these nanodots. The nanodots was scraped from the substrate and ultrasonically dispersed in ethanol. The suspension was dripped on a copper grid with carbon supporting films. After drying in air, the copper grid was placed in a transmission electron microscope (TEM, JEOL and JEM-2010) for lattice structure analyses. The chemical composition of these nanodots was determined by energy dispersive X-ray spectroscopy (EDS) attached to the TEM.

3. Results and discussion

According to PSIA mechanism [31,32], the concentrations of TBOT and PVP in the precursor sol could control nanodots morphology (size and density). Generally, the increase of the concentration of TBOT would produce larger TiO_2 nanodots because the mass accumulation of TBOT-rich droplets was triggered after the phase separation. Higher PVP concentration could lead dots to have smaller size and higher density because a larger surface tension gradient and a more intense convective flow were resulted. During this process, if Pb was incorporated into the TBOT-rich droplets, PT nanodots may form after subsequent calcination. Hence, the homogeneous incorporation of Pb into TBOT-rich droplets became the key point. It was reported that Hacac could effectively coordinated Pb ions into TBOT based gels and led to homogeneous tetragonal PT phase [34]. However, since PSIA is very sensitive to sol composition, the effects of Hacac addition on PSIA needed to be firstly investigated.

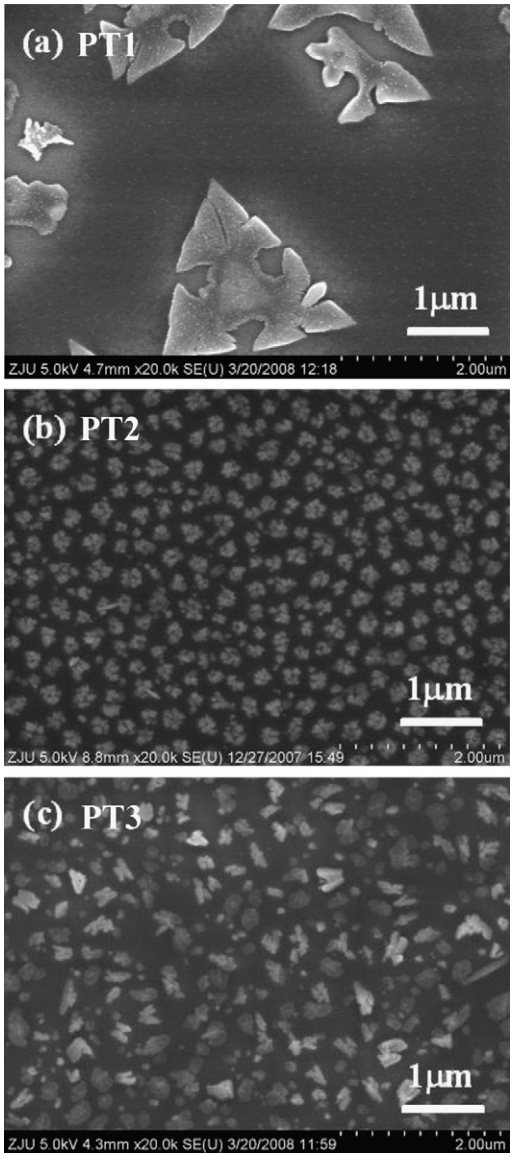

Fig. 1. Effects of Pb/Hacac molar ratio on phase separation.

Fig. 1 shows the effects of Hacac amount on morphology of samples (PT1, PT2 and PT3). Obviously, a small amount of Hacac only led to a few micrometer scale triangle flakes (Fig. 1a). With the increase of Hacac amount, nanodots agglomerates (Fig. 1b) and irregular nanoflakes appeared. These results indicated that Hacac did affect the phase separation process, besides the expected coordination with Pb. Within all the value tested, Pb:Hacac equaled to 1:2 seemed the most appropriate for nanodots formation.

In Fig. 2, the high-resolution TEM image and EDS spectrum of the obtained nanodots (PT2) were given. Lattices belonged to pure PT (JCPDS 6-452) were observed, indicating a perovskite

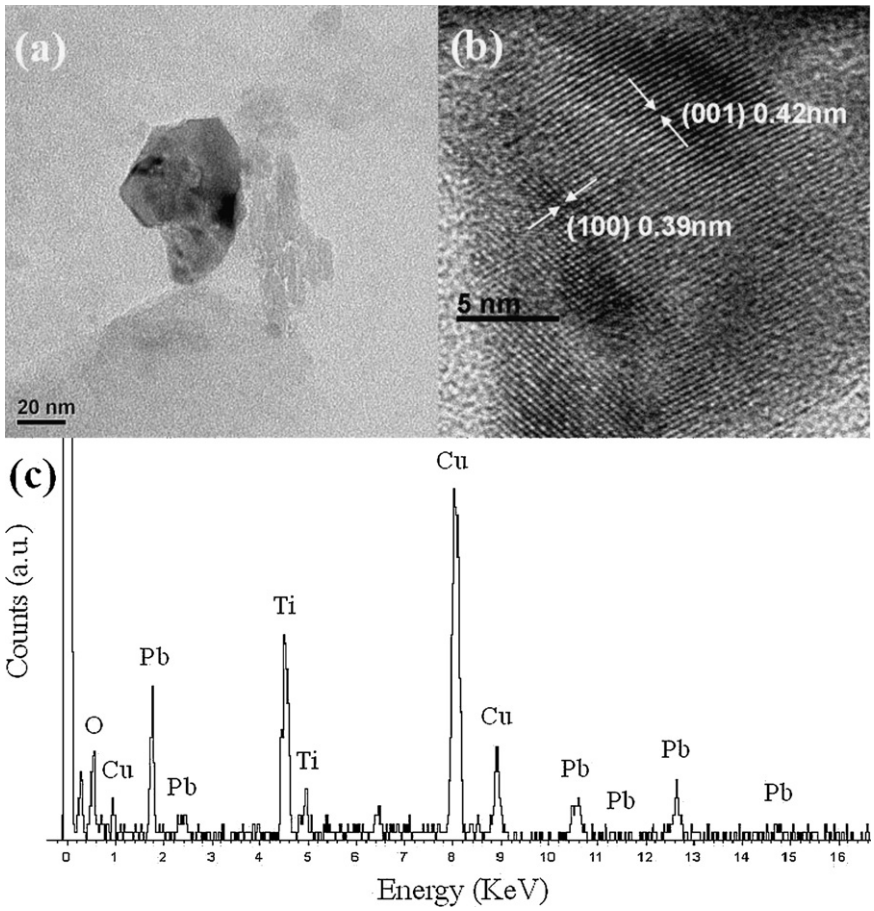

Fig. 2. TEM micrograph, HRTEM image and EDS spectrum of an individual nanodot on PT2. (a) TEM micrograph; (b) HRTEM image; (c) EDS spectrum.

structure of the nanodots. Also, Ti, O and Pb elements were identified in Fig. 2c (Cu, C and Si peaks in the EDS spectrum could be attributed to the supporting copper grid and Si substrate). Obviously, the nanodots obtained were PT perovskite phase.

Nevertheless, the obtained nanodots still existed as agglomerates. That meant the concentration of TBOT was basically too high. After reducing the TBOT concentration, the effects of concentration on PT nanodots were further investigated, as shown in Fig. 3. When the concentration of TBOT decreased from 0.03 mol/L to 0.005 mol/L in the precursor sol, smaller and denser PT nanodots tended to form. Image analysis showed that all the samples had rather narrow and controllable nanodots size distribution. With increasing TBOT concentration, the dominant nanodots size were around 20 nm, 20–30 nm, 50 nm and 70 nm respectively. While the corresponding nanodots density decreased from 4.6×10^{10}, through 3.6×10^{10} and 0.9×10^{10}, to 0.5×10^{10} dots/cm^2 on Si substrates (PT4, PT5, PT6 and PT7).

Besides the concentrations of TBOT, concentrations of PVP also influenced the formation of PT nanodots when the TBOT concentration was fixed. In Fig. 4, with the concentration of PVP increased from 20 g/L to 40 g/L, the average size of PT nanodots decreased from 60 to 45 nm, and the density increased from 0.4×10^{10} to 1.4×10^{10} dots/cm^2 (PT8, PT6 and PT9).

Obviously, both TBOT concentrations and PVP concentrations affected the size and density of nanodots. However, their effects showed much difference: TBOT concentration affected both nanodots size and density, while PVP concentration mainly affected nanodots density, only a slight effect on nanodots size was observed. In fact, conferring to the formation of TiO_2 nanodots on substrate [32], PT nanodots formation could be briefly summarized as following: a liquid film firstly forms, then phase separation occurs through the convective flows of (Pb, Ti)-rich and (Pb, Ti)-poor phases (PVP). Thus (Pb, Ti)-rich precursor nanodots form on the surface. After heat treatment, crystalline PT nanodots are obtained. For TBOT, a higher concentration usually means a thicker liquid film, stronger convective flow (thus accumulated into larger but fewer precursor nanodots after phase separation) and less shrinkage after annealing. These changes may eventually lead to larger but sparser nanodots. As for PVP, at a given TBOT concentration, a higher concentration means less convective flow and more PVP to separate those (Pb, Ti)-rich precursor nanodots. As a result, sparser nanodots form. Since the size of nanodots is mainly influenced by the extent of convective flow, the effect of PVP concentration on nanodots size is rather moderate.

In general, in this precursor system, it seemed easy to incorporate ions to form titanate nanodots on Si surface. It is expected that nanodots of other titanate materials, such as lead zirconium titanate and barium titanate, could be easily obtained through similar routes.

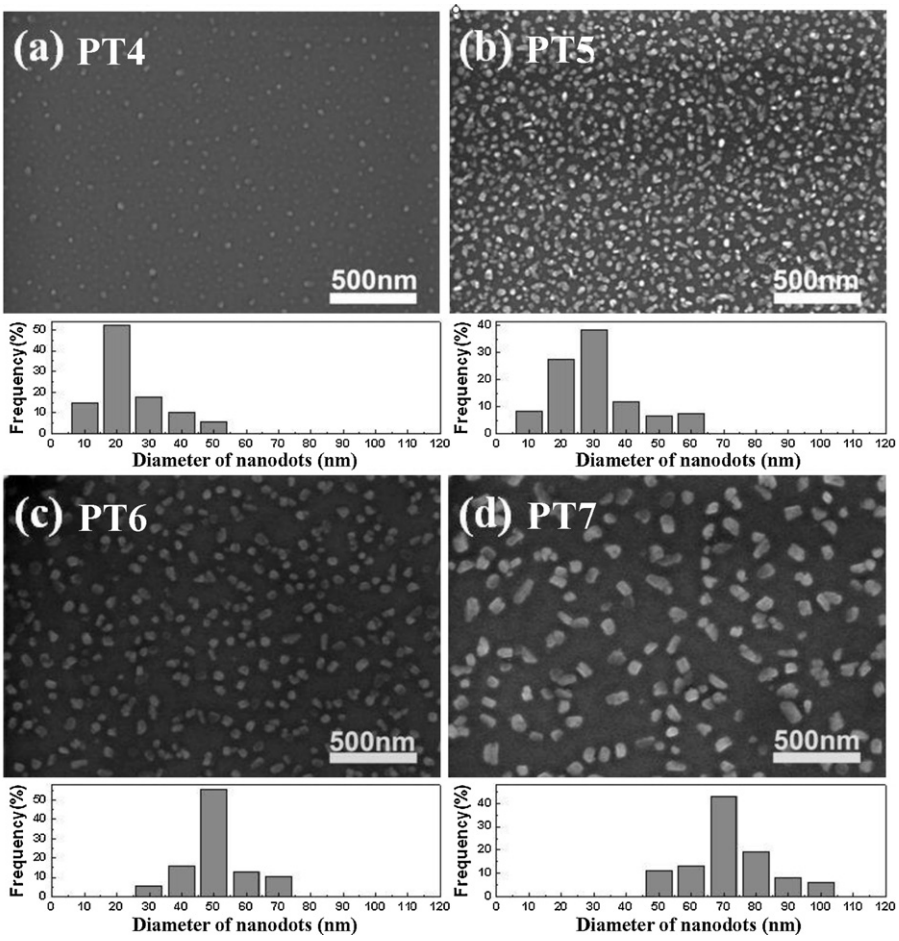

Fig. 3. Effects of TBOT concentration on nanodots size, density and size distribution.

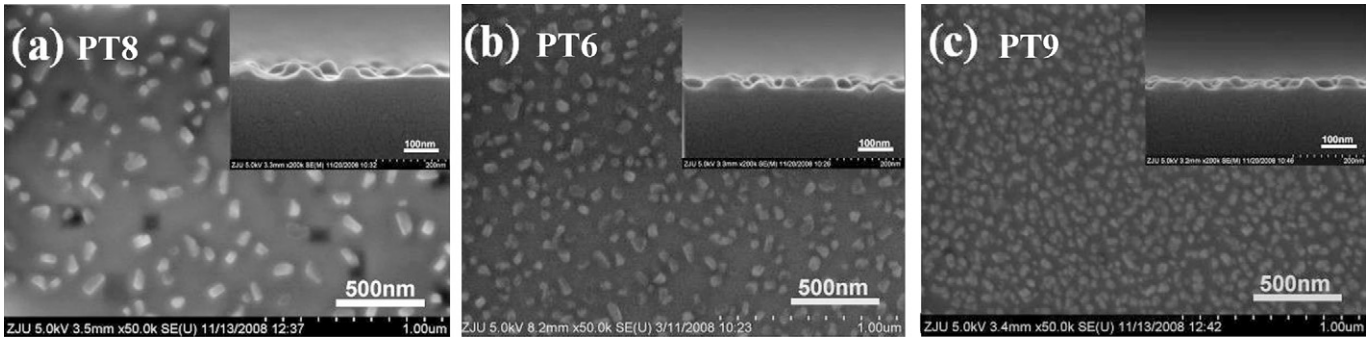

Fig. 4. Effects of PVP amount on nanodots density (insets are cross-section views).

4. Conclusions

PT nanodots on Si substrate with controlled size and density could be formed through a PSIA way. The nanodots showed a perovskite structure. It is concluded that TBOT concentrations could affect the nanodots size and density simultaneously, from around 20 nm, 4.6×10^{10} dots/cm^2, to 70 nm, 0.9×10^{10} dots/cm^2; at a fixed TBOT concentration, the variation of PVP amount could also affect the density of nanodots.

Acknowledgments

The work is financially supported by National Science Foundation of China (NSFC, grant no. 30870627 and 51072178).

References

[1] Z.H. Zhu, Z.G. Liu, N.B. Ming, J. Mater. Chem. 20 (2010) 4015–4030.
[2] J.H. Zhang, S.J. Mo, H.Y. Wang, S.X. Zhen, H.W. Chen, C.R. Yang, J. Alloys Compd. 509 (2011) 2838–2841.
[3] Z.Y. Shen, J.F. Li, J. Ceram. Soc. Jpn. 118 (2010) 940–943.
[4] W.Z. Lu, Y. Wang, G.F. Fan, X.H. Wang, F. Liang, J. Alloys Compd. 509 (2011) 2738–2744.
[5] A. Ullah, C.W. Ahn, A. Hussain, S.Y. Lee, J.S. Kim, I.W. Kim, J. Alloys Compd. 509 (2011) 3148–3154.
[6] H.Q. Wang, R.Z. Zuo, J. Fu, Y. Liu, J. Alloys Compd. 509 (2011) 936–941.
[7] A. Ruediger, R. Waser, J. Alloys Compd. 449 (2008) 2–6.
[8] B. Jiang, J.L. Peng, L.A. Bursill, W.L. Zhong, J. Appl. Phys. 87 (2000) 3462–3467.
[9] H.M. Jang, T.Y. Kim, I.W. Park, Solid State Commun. 127 (2003) 645–648.
[10] O. Khamman, R. Wongmaneerung, W. Chaisan, R. Yimnirun, S. Ananta, J. Alloys Compd. 456 (2008) 492–497.
[11] E.R. Camargo, C.M. Barrado, C. Ribeiro, E. Longo, E.R. Leite, J. Alloys Compd. 475 (2009) 817–821.

[12] S.M. Selbach, G.Z. Wang, M.A. Einarsrud, T. Grande, J. Am. Ceram. Soc. 90 (2007) 2649–2652.
[13] S.W. Liu, Z.L. Xiu, J. Liu, F.X. Xu, W.N. Yu, J. Pan, X.P. Cui, H.X. Yu, J. Alloys Compd. 441 (2007) L7–L9.
[14] R. Wongmaneerung, A. Rujiwatra, R. Yimnirun, S. Ananta, J. Alloys Compd. 475 (2009) 473–478.
[15] Y.G. Wang, G. Xu, L.L. Yang, Z.H. Ren, X. Wei, W.J. Weng, P.Y. Du, G. Shen, G.R. Han, J. Alloys Compd. 481 (2009) L27–L30.
[16] M.C. Hsu, I.C. Leu, Y.M. Sun, M.H. Hon, J. Solid State Chem. 179 (2006) 1421–1425.
[17] L. Liu, T. Ning, R. Yan, Z. Sun, F. Wang, W. Zhou, S. Xie, L. Song, S. Luo, D. Liu, S. Jun, W. Ma, Y. Zhou, Mater. Sci. Eng. B-Adv. Funct. Solid-State Mater. 149 (2008) 41–46.
[18] Y. Yang, X.H. Wang, C.K. Sun, L.T. Li, J. Am. Ceram. Soc. 91 (2008) 3792–3794.
[19] S.G. Lee, Y.J. Shim, C.J. Kim, J.K. Chung, J. Alloys Compd. 449 (2008) 73–76.
[20] H. Nonomura, M. Nagata, H. Fujisawa, M.A. Shimizu, H. Niu, K. Honda, Appl. Phys. Lett. 86 (2005) 163106.
[21] I. Szafraniak, C. Harnagea, R. Scholz, S. Bhattacharyya, D. Hesse, M. Alexe, Appl. Phys. Lett. 83 (2003) 2211–2213.
[22] J. Wang, X.C. Pang, M. Akinc, Z.Q. Lin, J. Mater. Chem. 20 (2010) 5945–5949.
[23] M. Torres, J. Ricote, L. Pardo, M.L. Calzada, Integr. Ferroelectr. 99 (2008) 95–104.
[24] M.L. Calzada, M. Torres, J. Ricote, L. Pardo, J. Nanopart. Res. 11 (2009) 1227–1233.
[25] Y.K. Kim, H. Han, Y.S. Kim, W. Lee, M. Alexe, S. Baik, J.K. Kim, Nano Lett. 10 (2010) 2141–2146.
[26] J. Chen, X.R. Xing, R.B. Yu, J.X. Deng, G.R. Liu, J. Alloys Compd. 388 (2005) 308–313.
[27] W. Sakamoto, Y. Masuda, T. Yogo, J. Alloys Compd. 408–412 (2006) 543–546.
[28] M. Feng, W. Wang, H. Ke, J.C. Rao, Y. Zhou, J. Alloys Compd. 495 (2010) 154–157.
[29] P.A. Shaikh, R.C. Kambale, A.V. Rao, Y.D. Kolekar, J. Alloys Compd. 486 (2009) 442–446.
[30] S.H. Leal, M.T. Escote, F.M. Pontes, E.R. Leite, M.R. Joya, P.S. Pizani, E. Longo, J.A. Varela, J. Alloys Compd. 475 (2009) 940–945.
[31] M. Luo, K. Cheng, W.J. Weng, C.L. Song, P.Y. Du, G. Shen, G. Xu, G.R. Han, Nanotechnology 20–21 (2009) 215605.
[32] M. Luo, K. Cheng, W.J. Weng, C.L. Song, P.Y. Du, G. Shen, G. Xu, G.R. Han, J. Phys. D-Appl. Phys. 42 (2009) 7.
[33] J.N. Li, M. Luo, W.J. Weng, K. Cheng, P.Y. Du, G. Shen, G.R. Han, Appl. Surf. Sci. 256 (2009) 342–345.
[34] I. Arcon, B. Malic, M. Kosec, A. Kodre, Mater. Res. Bull. 38 (2003) 1901–1906.